

## Syntheses, volume, and structural changes of garnets in the pyrope-grossular join: Implications for stability and mixing properties

JIBAMITRA GANGULY, WEIJI CHENG

Department of Geosciences, University of Arizona, Tucson, Arizona 85721, U.S.A.

HUGH ST.C. O'NEILL

Bayerisches Geoinstitut, Universität Bayreuth, D-8580 Bayreuth, Germany

### ABSTRACT

We have synthesized 11 garnet compositions in the pyrope-grossular join from glass starting materials by a combination of hydrothermal synthesis and recycling of most of the products at  $\sim 40$  kbar,  $1400^\circ\text{C}$ , in graphite capsules. Syntheses of homogeneous crystals were also successful within the compositional range  $\text{Gr}_{50}\text{--Gr}_{80}$ , which represented a conspicuous gap in earlier studies on synthetic garnets.

The lattice parameters of the synthetic garnets have been determined with a precision of  $0.0002\text{--}0.0004$  Å. The results show a slightly positive excess volume of mixing, which is asymmetric toward the grossular end, and can be described by a subregular or Margules formulation with  $W_{\text{CaMg}}^V = 0.36 \pm 0.23$  and  $W_{\text{MgCa}}^V = 1.73 \pm 0.3$   $\text{cm}^3/\text{mol}$  (12 O atom basis). Powder X-ray diffraction (XRD) structural refinements show linear dependence of the O positional parameters and cation to O distance in dodecahedral, octahedral, and tetrahedral sites on the Ca content of garnet.

The partial molar volume of grossular in pyrope-grossular and almandine-grossular joins, determined from our data and those of Geiger et al. (1989), varies smoothly and similarly between the terminal compositions and exceeds the molar volume by  $<1\%$ , which has an effect of no more than  $1.5\%$  on the calculation of equilibrium pressure of the assemblage grossular + aluminosilicate + plagioclase + quartz. The partial molar volumes of pyrope and almandine change very similarly as a function of the Ca content of garnet. The  $V$ - $X$  relation of the pyrope-grossular join determined in this work has been used to calculate the effect of lattice strain on the enthalpy of mixing. We have also extended the formulation of Ferreira et al. to derive a simple but general expression to account for the effect of multiautom interaction on lattice strain.

### INTRODUCTION

Most mineralogical equilibria that are commonly used as geothermometers and geobarometers involve garnet as one of the phases. Calibration of these equilibria as  $P$ - $T$  sensors requires a thorough understanding of the thermodynamic mixing property of garnet solid solution at least within the range of compositions commonly encountered in the natural assemblages. The present paper is part of a continuing project in the development of a comprehensive solution model of aluminosilicate garnet solid solution in the Ca-Mg-Fe-Mn quaternary system, and it deals primarily with the syntheses of garnets and experimental determination of volume change in the pyrope-grossular join, along with its thermochemical implications.

Haselton and Newton (1980) and Newton and Wood (1980) concluded that the molar volume in the pyrope-grossular binary has an S-shaped form, with a small negative deviation near the pyrope end (also see Delaney,

1981) and a somewhat larger positive deviation toward the grossular end. (A very similar volumetric behavior was reported by Cressey et al., 1978, for the almandine-grossular binary.) Subsequently Wood (1988) made several additional measurements on synthetic pyrope-grossular solid solution and regressed the data along with the others to suggest a small asymmetric positive deviation from ideality toward the grossular end, but without a negative deviation near the pyrope end. Berman (1990) reviewed the available data on garnet solid solution and concluded that the "excess volumes in the grossular-pyrope join are poorly constrained by the data." He argued that the scatter of the data is too large to justify the use of anything but the simplest mixing model and thus fitted the available volume data by a symmetrical nonideal model. The various excess volume models, along with the available experimental data, are illustrated in Figure 1. The experimental data are taken directly from the compilation of Berman (1990). It is evident that the data are too scattered to lead to a reliable model. Further,

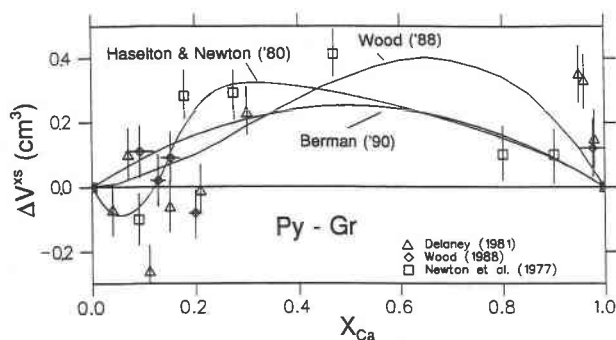


Fig. 1. Excess molar volume data in the pyrope-grossular join, as compiled by Berman (1990), along with the various models fitted to part or all of the data.

there is a conspicuous gap of data between  $\sim 50$  and  $80$  mol% grossular composition. This gap, which is also present in the calorimetric enthalpy data in the pyrope-grossular join (Newton et al., 1977), is a consequence of the failure to synthesize homogeneous garnets that have composition within the above range.

We report in this work syntheses of homogeneous garnet crystals in the pyrope-grossular join, including the gap between  $50$  and  $80$  mol% grossular content, and careful independent measurements of cell volumes of these synthetic crystals, which would remove the ambiguity of the excess volume model in this join. We have also carried out structural investigation by the Rietveld method on several of the synthetic samples and calculated the contribution of elastic strain caused by solid solution on the enthalpy of mixing.

### EXPERIMENTAL PROCEDURE

Garnets of all compositions in the pyrope-grossular join were synthesized from glasses in a piston cylinder apparatus. First end-member glasses were prepared by melting stoichiometric oxide mixtures. Glasses of intermediate compositions were prepared by remelting finely ground mixtures of the end-member glasses.

#### Preparation of glasses

The following oxides were used to prepare end-member glasses: MgO [Johnson and Mathey (JM) puratronic],  $\text{CaCO}_3$  (Baker,  $>99.98\%$  pure),  $\gamma\text{-Al}_2\text{O}_3$  (JM puratronic),  $\text{SiO}_2$  (Alfa Co.,  $99.9\%$  pure). All starting oxides were dried at  $110^\circ\text{C}$  prior to weighing. Five grams of both end-member oxide compositions were mixed manually under alcohol for about 1 h and then further homogenized in a SPEX vibrating mixture for 20 min. The grossular mixture, in which  $\text{CaCO}_3$  was used as the source for Ca, was fired at  $800^\circ\text{C}$  for 4 h after preparation of the stoichiometric oxide mixture to remove  $\text{CO}_2$  before melting. The oxide mixtures were melted in a Deltech  $\text{MoSi}_2$  furnace for about 45 min to 1 h and quenched. Microprobe analyses of the end-member and a few selected intermediate glasses showed them to be homogeneous to within  $\pm 3\%$

( $\pm 2\sigma$ ) of the average composition. The temperatures at which the oxide mixtures were melted are as follows: pyrope:  $1620^\circ\text{C}$ ; grossular:  $1400^\circ\text{C}$ ;  $\text{Py}_x\text{Gr}_{1-x}$ :  $1450\text{--}1580^\circ\text{C}$ , depending on the composition. The end-member mixtures were melted in Pt crucibles, whereas the intermediate ones were melted in graphite crucibles under Ar atmosphere (to prevent the graphite crucible from burning off). The graphite flakes were burned off the glasses by heating at  $500^\circ\text{C}$  for 2 h in air (there was no special reason for choosing graphite crucible for the intermediate mixtures except convenience).

#### Synthesis of garnets

The synthesis conditions and results are summarized in Table 1. Pyrope and grossular were synthesized hydrothermally in a piston cylinder apparatus using a pressure vessel fitted with a carbide core  $\frac{3}{4}$  in. in diameter. Glasses of the respective compositions were sealed (without any seed crystal) with approximately  $20\text{--}30$  wt% distilled  $\text{H}_2\text{O}$  in Au capsules 3 mm in diameter and were held at 25 kbar,  $1000^\circ\text{C}$ , for 20 h in a pressure cell with CsCl outer bushing. The products were 100% pure garnets (within the limits of detection by optical and X-ray methods) with crystal sizes ranging from  $\sim 200$  to  $400\ \mu\text{m}$ . Dry synthesis of pyrope at 25 kbar,  $1200^\circ\text{C}$ , for 20 h with 7 wt% pyrope seed was not completely successful; the product had  $\sim 5\%$  extraneous phases.

Syntheses of garnets of intermediate compositions have been complicated by the fact that in the system  $\text{CaSiO}_3\text{--MgSiO}_3\text{--Al}_2\text{O}_3$  (CMA), the clinopyroxene join  $\text{CaAl}_2\text{SiO}_6\text{--CaMgSi}_2\text{O}_6$  (CTs-Diop) can pierce the grossular-pyrope join, depending on the  $P\text{--}T$  condition, thus rendering intermediate garnet unstable relative to pyroxene (Boyd, 1970). This explains the lack of any mixing property data for garnets in the compositional range  $\text{Gr}_{50}\text{--Gr}_{80}$ . Higher pressure or lower temperature are expected to stabilize garnet relative to clinopyroxene. Prior to microprobe analysis, all experimental products were checked for the homogeneity of garnet composition and the presence of extraneous phases by XRD scan using Cu radiation. The extent of splitting of the  $K\alpha_1$  and  $K\alpha_2$  doublet above  $50^\circ 2\theta$  value was found to be a good indicator of the homogeneity of the garnet composition. Microprobe analysis of garnets, for which the 642 reflection was clearly separated into the  $\alpha_1$  and  $\alpha_2$  doublet, always showed homogeneity of composition within  $\pm 0.5\%$ .

We found that the best way to synthesize homogeneous garnet with  $\sim 100\%$  yield was first to perform a hydrothermal synthesis at  $\sim 25$  kbar,  $1000^\circ\text{C}$ , for 25 h, then grind (grain size  $5\text{--}10\ \mu\text{m}$ ) and remix the product in an agate mortar and recycle it at  $40\text{--}42$  kbar,  $1350\text{--}1400^\circ\text{C}$ , for  $\sim 48$  h under dry conditions if there was any extraneous phase or the garnet was heterogeneous in composition, as indicated by the poor resolution of the  $\alpha_1\text{--}\alpha_2$  doublet. An example is shown in Figure 2. Here the product JW/7 ( $\text{Gr}_{54}$ ) showed broad reflections with only partial separation of the doublets, indicating heterogeneity

**TABLE 1.** Summary of selected experimental data for syntheses of pyrope-grossular garnet solid solutions

Expt.*	Starting material	Conditions			Results**
		<i>P</i> (kbar)	<i>T</i> (°C)	<i>t</i> (h)	
JW/16	glass	25	1000	24	Gt, 40–50 μm, heterogeneous
JW/25	product of JW/16	40	1400	48	Gt, ~60 μm, $X_{Ca} = 0.073(3)$
JW/14	glass	25	1000	20	Gt, 60–100 μm, heterogeneous
JW/30	product of JW/14	40	1400	48	Gt, $X_{Ca} = 0.134(3)$
JW/13	glass	25	1000	20	Gt, ~50 μm, $X_{Ca} = 0.196(8)$
JW/17	glass	25	1000	24	Gt, ~5% CPx, ~1% others
JW/28	product of JW/17	40	1400	48	Gt, ~30 μm, $X_{Ca} = 0.258(4)$
JW/18	glass	25	1000	24	Gt, ~5% CPx
JW/29	product of JW/18	40	1400	48	Gt, $X_{Ca} = 0.384(7)$
JW/19	glass	42	1000	24	Gt, ~15 μm, ~5% CPx
JW/26	product of JW/19	40	1400	48	Gt, ~15 μm, <3% others, $X_{Ca} = 0.491(1)$
JW/31	product of JW/19 +3% of JW/29 as seed	40	1400	48	Gt, ~3% others, $X_{Ca} = 0.473(7)$
JW/07	glass	25	1000	25	Gt, ~20 μm, heterogeneous
JW/21	product of JW/07	40	1400	48	Gt, ~20 μm, $X_{Ca} = 0.536(3)$
JW/20	glass	42	1000	24	Gt, 20–40 μm, heterogeneous
JW/22	product of JW/20	40	1400	48	Gt, $X_{Ca} = 0.702(3)$
JW/03	glass	30	1000	12	Gt, ~35 μm, $X_{Ca} = 0.797(2)$
JW/15	glass	25	1000	20	Gt, $X_{Ca} = 0.849(3)$ ; 22 analyses
JW/23	glass (Gr <sub>20</sub> Py <sub>80</sub> )	40	1350	48	Gt, 5–8% others

Note: All experiments at 1000 °C were in Au capsules sealed with H<sub>2</sub>O; others were in graphite capsules (dry).

\* The experiments are arranged in the order of increasing Ca content ( $X_{Ca}$ ).

\*\* Stated garnet (Gt) compositions represent average of 12–14 analyses, except for experiment no. JW/15.

of composition. The latter was, therefore, recycled (JW/21) as described above, which resulted in sharp X-ray reflections with clear separation of the  $\alpha_1$ - $\alpha_2$  doublet. Hydrothermal experiments at 25 kbar, 1000 °C, yielded homogeneous garnet when the grossular content exceeded 80 mol%. Attempts to synthesize homogeneous garnets with lower grossular content directly through dry experiment at 40 kbar were not successful (e.g., experiment JW/23).

We have illustrated in Figure 3 the compositions of synthetic garnets on the CMA phase diagram of Boyd (1970) at 30 kbar. Boyd's original diagram is in weight percent and has been recast in terms of mole percent of the components. All experiments that are indicated by circle, excepting the one with garnet composition Gr<sub>70</sub> (experiment JW/22), yielded single phase garnet under hydrothermal condition at 25–30 kbar, 1000 °C, 25 h. Of these, the products of the experiments JW/3 (Gr<sub>0.80</sub>) and JW/15 (Gr<sub>0.85</sub>) were very homogeneous and therefore did not require any recycling. The experiment JW/22 was under hydrothermal condition at 40 kbar, 1000 °C, and also yielded single phase garnet (Gr<sub>70</sub>). We believe, after reviewing the results of all synthesis experiments, that garnet with Gr<sub>70</sub> composition can be synthesized hydrothermally at 25 kbar, 1000 °C (also see Gasparik, 1984). The products of the experiments indicated by a triangle in Figure 3 (experiment JW/17 and JW/29) showed small but significant amounts of clinopyroxene, along with other extraneous phases, after hydrothermal syntheses at 25 kbar, 1000 °C, but these phases disappeared after the products were recycled at the higher *P-T* condition, as

described above. However, we failed to synthesize single phase well-crystallized garnet of composition Gr<sub>50</sub> (experiment JW/19 and JW/26), which is suitable for precise cell dimension measurement.

### Microprobe analysis

All synthetic garnet solid solutions were analyzed in a Cameca SX50 electron microprobe at the University of Arizona, using an accelerating voltage of 15 kV and a beam current of 30 nA. X-rays were collected for 30 s on each spot. Synthetic end-member pyrope and grossular garnets were used as standards. The composition of each sample reported in Table 1 represents an average of 11–14 spot analyses, except for the product of experiment JW/15. It represents an average of 22 spot analyses made in two independent sessions because of the anomalous cell volume of the garnet, as discussed later.

### X-RAY DIFFRACTION STUDIES

#### Lattice parameter and excess volume measurements

Lattice parameters were measured using CoK $\alpha_1$  radiation ( $\lambda = 1.78897 \text{ \AA}$ ) on a STOE STADIP focusing diffractometer with a curved Ge monochromator. The diffractometer operates with a flat, rotating sample in the transmission geometry mode and is equipped with a position-sensitive detector, with an operating width of about 8°  $2\theta$ . All samples were measured with an internal Si standard from the U.S. National Bureau of Standards (NBS). The diffraction pattern was collected from 61 to 141°  $2\theta$ ,

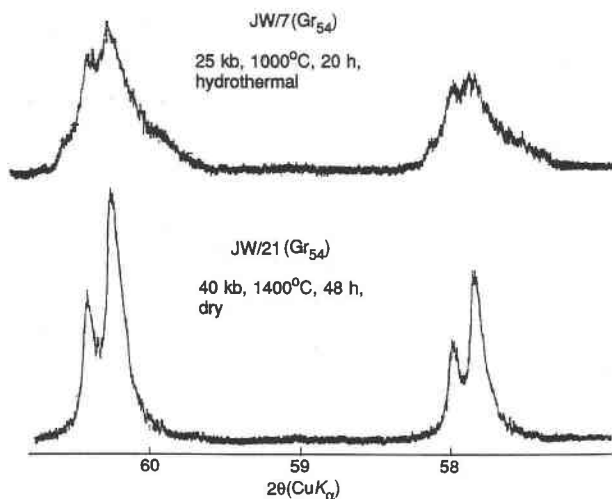


Fig. 2. X-ray diffractometer scans (Cu radiation) of synthetic garnets, illustrating the distinctive effect of compositional heterogeneity on the resolution of  $K\alpha_1$ - $\alpha_2$  doublet around  $60^\circ 2\theta$ . The product of experiment JW/7 (20 kbar, 1000 °C, 20 h, hydrothermal) showed poor resolution caused by compositional heterogeneity, but the resolution improved greatly on recycling the product to 40 kbar, 1400 °C, for 48 h.

using  $1/2^\circ$  increments of the position-sensitive detector. Proprietary software from STOE was used to determine peak positions by fitting entire peak profiles. The six Si peaks in the  $2\theta$  range covered were used to derive a two-term (linear) correction to the observed values of  $2\theta$ . The lattice parameter was then determined by a weighted nonlinear least-squares refinement of the positions of the 12–15 most intense reflections (except for samples with a bimodal population of compositions, for which only those highest angle reflections in which the different populations were resolved were used—see below). The peak positions were weighted according to the estimated standard deviation from the peak profile fitting. The results are given in Table 2. The estimated uncertainties include not only those found from the least-squares procedure, but also those from fitting the internal standard, as well as an estimated contribution from the effects of thermal expansion and variation in laboratory temperature. It is to be noted that the relative error in the lattice parameter measurements is  $<0.1\%$  of the variation across the solid solution and is therefore proportionately less than the uncertainty in the composition.

For most samples the relatively narrow peak half-widths (approaching those of the Si internal standard) confirm the high degree of compositional homogeneity found by electron microprobe analysis. Three samples (JW13, JW27, and JW30) were found to consist of two discrete garnet compositions (Table 2). In each case, only the dominant composition was encountered during the microprobe analysis, suggesting that the subordinate composition might be finer grained. Although the bimodal nature of these samples was readily apparent from examination of the highest angle reflections, it could, in our

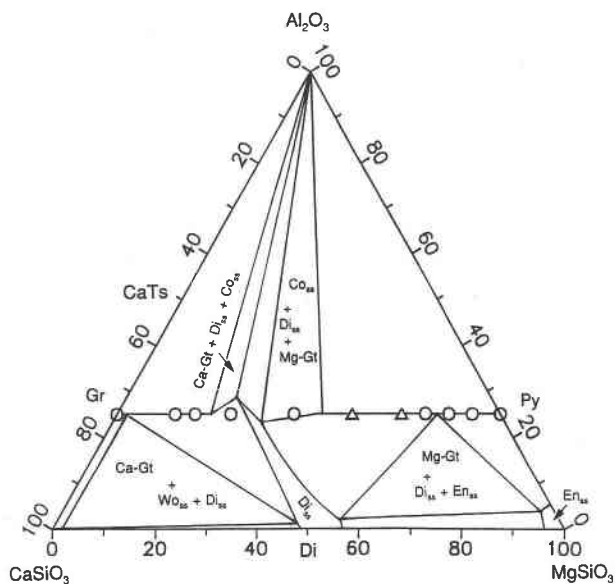


Fig. 3. Compositions of garnets in the pyrope-grossular join, synthesized in this work, compared with the phase diagram of Boyd (1970) in the system  $\text{CaSiO}_3$ - $\text{MgSiO}_3$ - $\text{Al}_2\text{O}_3$  (CMA) at 30 kbar, 1200 °C (Boyd's original diagram is in weight percent scale, which has been converted here to mole percent).  $\text{Co}_s$ : corundum solid solution;  $\text{Di}_s$ : diopside solid solution;  $\text{En}_s$ : enstatite solid solution. The unlabeled fields represent two phase fields consisting of garnet solid solution and one of the above phases. Circles indicate successful syntheses of single-phase garnet (but not necessarily homogeneous) under hydrothermal conditions at 25 kbar, 1000 °C, except the one with  $X_{\text{Ca}} = 0.70$  (experiment JW/20), which was at 42 kbar, 1000 °C, under hydrothermal condition. The triangles indicate that the products of hydrothermal syntheses at 25 kbar, 1000 °C, contained pyroxene and other phases, which disappeared on recycling at 40 kbar, 1400 °C, under dry condition, yielding single-phase homogeneous garnets.

opinion, easily have been overlooked if only lower angle ( $2\theta < 90^\circ$ ) reflections had been measured, or if unmonochromated  $\alpha_1 + \alpha_2$  radiation had been employed. In such cases the lattice parameter would be an average of the two populations, but the microprobe analysis might be that of the dominant population only.

Excess molar volumes were obtained by weighted least-squares fitting of the data in Table 2, first using a second-order polynomial (equivalent to a regular solution model), and then using a third-order polynomial (subregular or Margules model). The reduced  $\chi^2$  [ $\chi^2_r = \chi^2/(N - n - 1)$ ; Bevington, 1969, p. 202] for the regular solution model was 8.1, which is unacceptably high; for the subregular model,  $\chi^2_r$  decreased to 4.7, a significant improvement, but still high. Higher order expressions produced insignificant decreases in  $\chi^2_r$ . The high  $\chi^2_r$  was entirely due to one apparently anomalous datum, that for JW15 ( $X_{\text{Ca}} = 0.849$ ), which appeared to have too large a molar volume for its measured composition. Elimination of this datum from the regression gave  $\chi^2_r = 2.5$  for the regular solution model and  $\chi^2_r = 0.75$  for the subregular model. Thus, the subregular model provides a significantly better represen-

**TABLE 2.** Compositions, lattice parameters, and molar volumes of pyrope-grossular garnet solid solutions

Sample	Composition $X_{Ca}$	Lattice parameter (Å)	Molar volume ( $cm^3$ )	Com- ments
JW12	0.000(0)	11.4566(2)	113.195(6)	
JW25	0.073(3)	11.4883(2)	114.137(6)	
JW30	0.134(3)	11.5125(4)	114.860(12)	a
JW13	0.196(8)	11.5420(4)	115.745(12)	b
JW28	0.258(4)	11.5670(2)	116.499(6)	
JW27	0.384(7)	11.6156(4)	117.974(12)	c
JW21	0.536(3)	11.6800(2)	119.947(6)	
JW22	0.702(3)	11.7445(3)	121.945(9)	d
JW3	0.797(2)	11.7817(3)	123.107(9)	
JW15	0.849(2)	11.8063(3)	123.880(9)	
JW11	1.000(0)	11.8515(2)	125.308(6)	

Note: a = Two garnets, other  $a_0 = 11.492$ . Ratio of intensities is about 1:0.5. b = Two garnets, other  $a_0 = 11.481$ . Ratio of intensities is about 1:0.2. c = Two garnets, other  $a_0 = 11.568$ . Ratio of intensities is about 1:0.6. d = High-angle peaks show some asymmetry to high  $2\theta$ , indicating some zoning toward more Mg-rich compositions.

tation of the  $V$ - $X$  relationship in the pyrope-grossular join, and is, therefore, recommended in this work. The third-order regression, excluding JW15, led to the following expression of the molar volume of garnet on a 12 O atom basis:

$$V(\text{cm}^3) = 113.194 \pm 0.006 + 12.477(\pm 0.235)X_{Ca} + 1.002(\pm 0.604)X_{Ca}^2 - 1.36(\pm 0.380)X_{Ca}^3. \quad (1)$$

Reanalysis of JW15 by electron microprobe confirmed the initial analysis ( $0.848 \pm 0.002$  vs.  $0.850 \pm 0.002$ ; mean 0.849). The lattice parameter measurement was also repeated, first using the original mount and both Co and  $CuK\alpha_1$  radiations, and then with a second mount and Co radiation. The data from these experiments were also refined using the Rietveld method (see below). All measurements and both determination methods produced a lattice constant essentially identical to that determined initially. We are therefore unable to explain this anomaly at this stage, but further work is in progress to resolve this problem.

The  $V$ - $X$  relation in pyrope-grossular join is illustrated in Figure 4A, whereas the excess molar volumes ( $\Delta V^{XS}$ ), derived from Equation 1 and end-member volumes given in Table 2, are plotted vs. composition in Figure 4B. Only Wood's model (Wood, 1988; see Fig. 1 of this paper) is in qualitative agreement with our results. The error bars represent  $\pm 1\sigma$  and include the errors in the measurement of cell volumes of intermediate and end-member compositions.

#### Powder X-ray diffraction structural refinements

Several samples for which sufficient material was available to make a good mount were selected for further structural investigation by powder XRD. Most of these specimens already contained the Si internal standard, and in addition most contained detectable amounts of quartz and some the noble metal (Au or Pt) from the capsule.

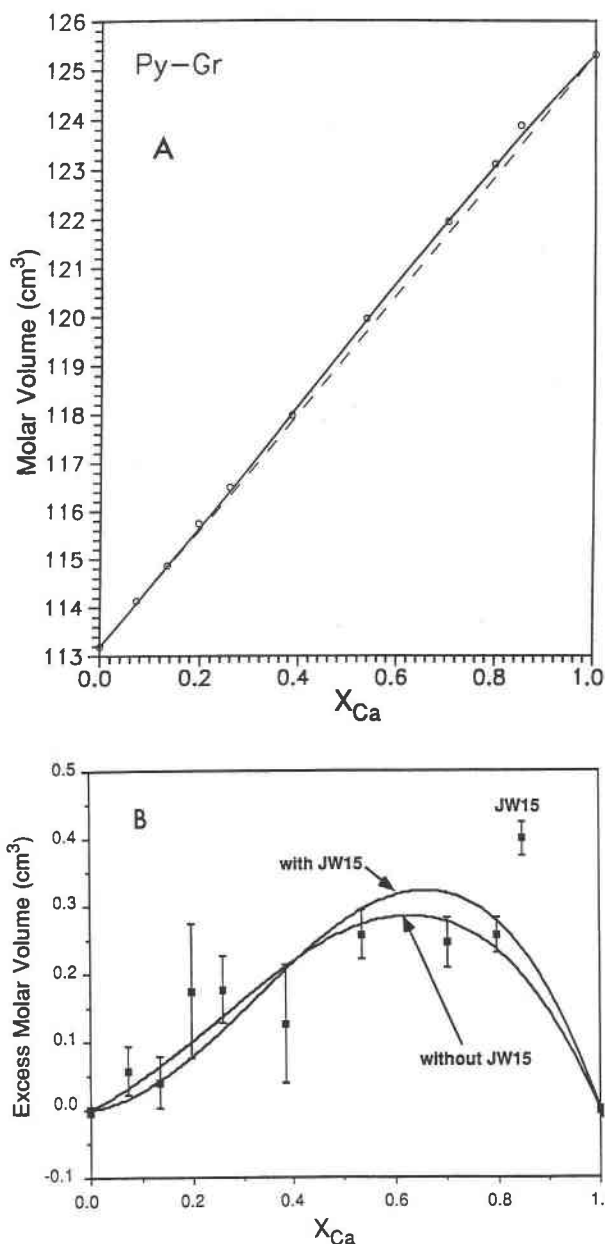


Fig. 4. (A) Molar volume and (B) excess molar volume vs. composition in the pyrope-grossular join, as determined in this work. The anomalous datum JW15 has been finally rejected. The error bars represent  $\pm 1\sigma$ . The molar volume data are precise to within the range  $\pm 0.006$  to  $\pm 0.012$   $cm^3$  (see Table 2).

Some samples also contained small amounts of another unidentified phase (either indigenous or from the pressure assembly used in the synthesis). Because this phase could not be satisfactorily accounted for in the refinement procedure, these samples produced inferior results and will not be considered further.

XRD data were collected using the same diffractometer as for the lattice parameter measurements, but with  $MoK\alpha_1$  radiation ( $\lambda = 0.709300$  Å). Five or six duplicate

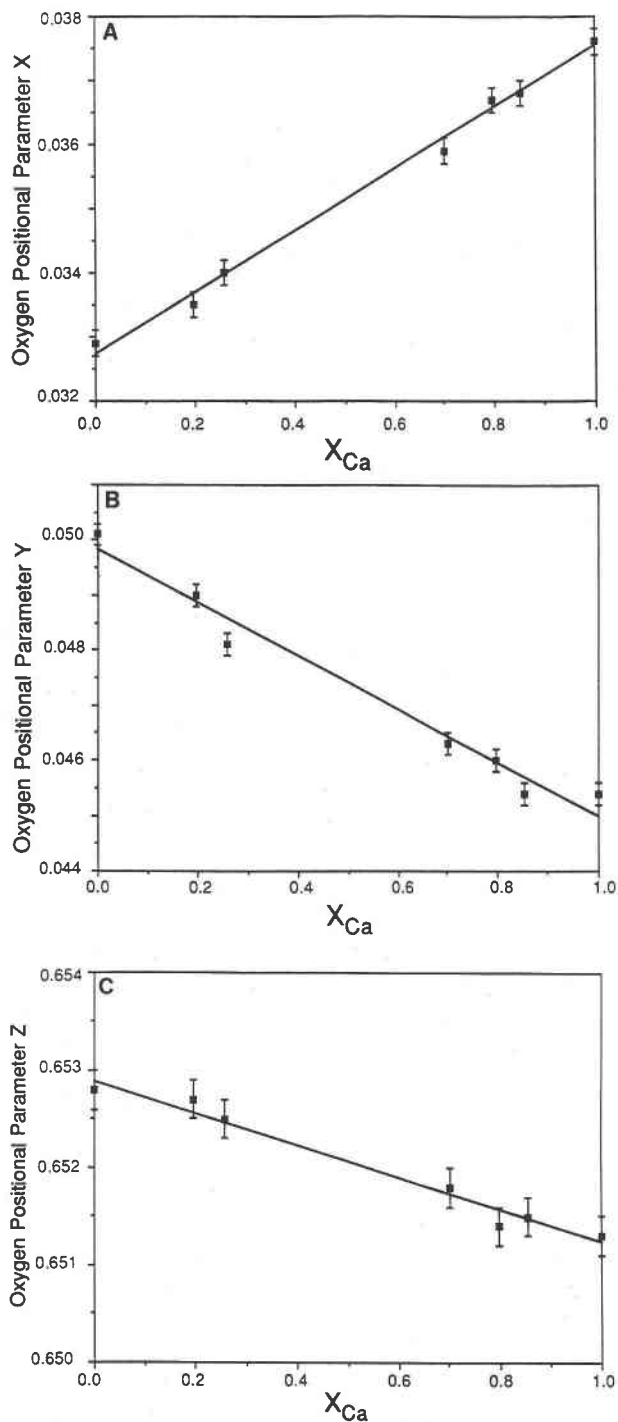


Fig. 5. O positional parameters  $x$  (A),  $y$  (B), and  $z$  (C) as a function of composition. All estimated standard deviations are 0.0002.

scans from 5 to  $88^\circ 2\theta$  [ $\sin(\theta/\lambda) = 0.98$ ] were collected for each sample and were checked for systematic drift in intensity. If that was negligible, the scans were summed to obtain the final powder diffraction pattern. Structures were refined by the Rietveld method, using the program DBW (version 3.2, locally modified; Wiles and Young, 1981).

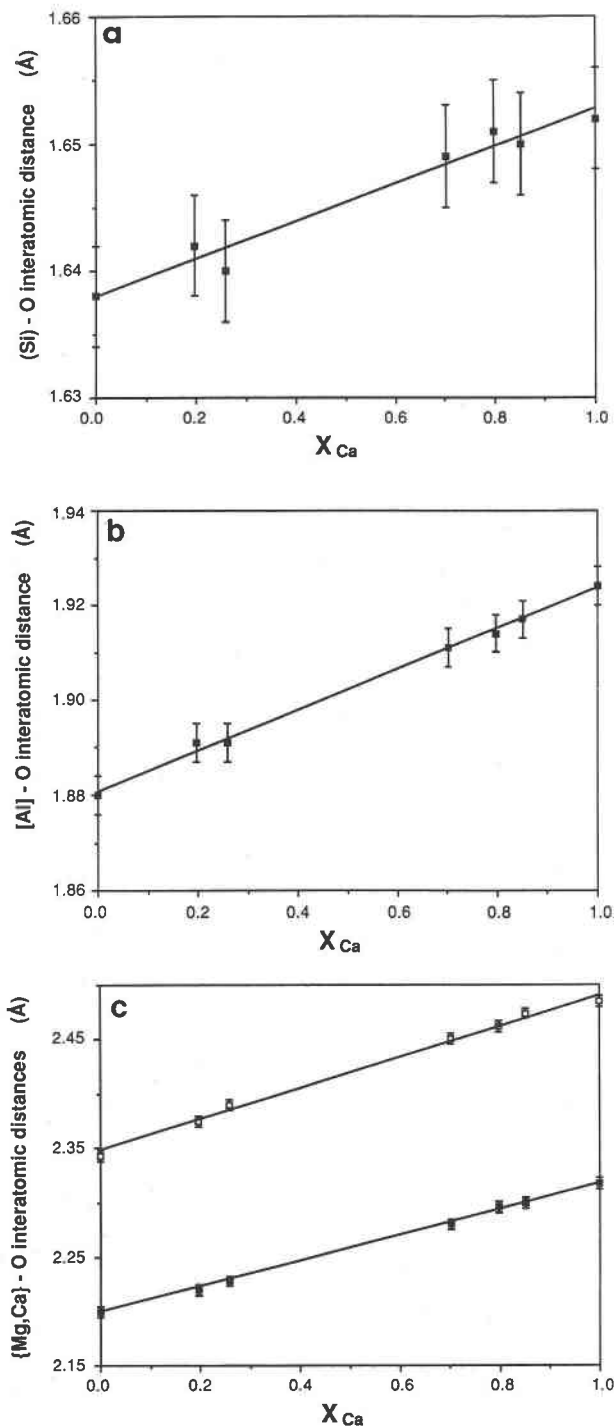


Fig. 6. Metal-O distance in the (a) dodecahedral, (b) octahedral, and (c) tetrahedral sites as a function of composition in the pyrope-grossular join. All uncertainties are 0.002 Å.

The structural model assumed space group  $Ia3d$  with complete occupancy of the 24  $c$  sites by Ca and Mg, the 16  $a$  sites by Al, the 24  $d$  sites by Si, and 96  $h$  sites by O. The ratio of Ca to Mg in the dodecahedral site was taken from the EMP analyses (Table 2). Refined parameters were a scale factor, the O atom positional param-

**TABLE 3.** Powder XRD structural refinements of garnets synthesized on the join  $Mg_3Al_2Si_3O_{12}$ - $Ca_3Al_2Si_3O_{12}$ 

Sample	Composi- tion $X_{Ca}$	O parameters*			Isotropic temperature factors ( $\text{\AA}^2$ )				$R_{Bragg}$	$R_F$
		$x$	$y$	$z$	$B_{dod}$	$B_{oct}$	$B_{tet}$	$B_{ox}$		
JW12	0	0.0329	0.0501	0.6528	0.707(45)	0.357(33)	0.293(31)	0.290(36)	6.44	8.08
JW13	0.196	0.0335	0.0490	0.6527	0.545(44)	0.135(33)	0.310(24)	0.215(43)	5.12	5.48
JW28	0.258	0.0340	0.0481	0.6525	0.579(29)	0.337(23)	0.395(26)	0.399(26)	4.92	5.98
JW22	0.702	0.0359	0.0463	0.6518	0.486(29)	0.297(27)	0.323(33)	0.216(30)	5.87	6.64
JW3	0.797	0.0367	0.0460	0.6514	0.423(35)	0.276(37)	0.383(46)	0.245(44)	6.14	7.68
JW15	0.849	0.0368	0.0454	0.6515	0.345(29)	0.222(33)	0.344(40)	0.191(39)	5.36	6.31
JW11	1	0.0376	0.0454	0.6513	0.323(21)	0.233(28)	0.265(31)	0.189(33)	4.73	5.62

\* All  $\pm 0.0002$  1 esd.

ters  $x$ ,  $y$ , and  $z$ , and the temperature factors. In order to keep the ratio of observations to structural variables reasonably high, a simple isotropic thermal motion model was employed, with separate isotropic temperature factors for each site (i.e.,  $B_{dod}$ ,  $B_{oct}$ ,  $B_{tet}$ , and  $B_{ox}$ ). Previous single-crystal refinements of pyrope and grossular (e.g., Novak and Gibbs, 1971) have shown that the thermal vibrations of the dodecahedral site atoms and the O atoms are in fact markedly anisotropic, but that using the approximation of the isotropic model produces no discernible error in the determination of the positional parameters. Profile functions were selected from experience with fitting spinel powder patterns (e.g., O'Neill et al., 1991). The quartz and noble metal impurity phases and the Si internal standard were treated similarly, using a single effective temperature factor for quartz and positional parameters constrained to literature values. The absorption for each sample was measured, and the absorption correction (which is virtually negligible) was made accordingly.

The results of structural refinement are summarized in Tables 3 and 4 and illustrated in Figures 5 and 6. The data for the end-member pyrope and grossular compare well with published data from single-crystal XRD studies. Within the limits of the uncertainty of the data, O positional parameters (Fig. 5) and cation to O distances in all three polyhedra (Fig. 6) show linear dependence on

composition. The results of structural refinement are not sufficiently precise to explain the nonlinear change of cell volume vs.  $X_{Ca}$ . The trends of compositional dependence of the structural parameters exhibited by the data in Figures 5 and 6 are in agreement with the observations of Novak and Gibbs (1971), who noticed these trends primarily from the results of structural refinements of end-member aluminosilicate garnets. They have cast their data in terms of mean radius of dodecahedral cations  $r\{X\}$ ; it is, however, easy to see that linear dependence against  $r\{X\}$  implies linear dependence against  $X$ .

The isotropic temperature factors for the octahedral, tetrahedral, and O sites do not show any significant variation with composition; mean values are  $B_{oct} = 0.27 \pm 0.08 \text{ \AA}^2$ ,  $B_{tet} = 0.33 \pm 0.05 \text{ \AA}^2$ , and  $B_{ox} = 0.25 \pm 0.08 \text{ \AA}^2$ . However,  $B_{dod}$  decreases from  $0.7 \text{ \AA}^2$  for pyrope to  $0.3 \text{ \AA}^2$  in grossular. These temperature factors agree reasonably well with those reported by Meagher (1975) and Hazen and Finger (1978).

#### IMPLICATIONS FOR THERMODYNAMIC MIXING PROPERTIES

##### Excess and partial molar volumes: Geothermobarometry

The excess molar volume data illustrated in Figure 4B can be expressed in terms of Margules formulation as

**TABLE 4.** O positional parameters and isotropic temperature factors of end-member pyrope and grossular

Reference	O positional parameters			Isotropic temperature factors ( $\text{\AA}^2$ )			
	$x$	$y$	$z$	$B_{dod}$	$B_{oct}$	$B_{tet}$	$B_{ox}$
<b>Pyrope (<math>Mg_3Al_2Si_3O_{12}</math>)*</b>							
Gibbs and Smith (1965)	0.0329(4)	0.0508(4)	0.6531(4)	0.67(8)	0.18(5)	0.13(4)	0.38(5)
Novak and Gibbs (1971)	0.0329(1)	0.0502(1)	0.6534(1)	0.79(3)	0.40(2)	0.19(2)	0.50(3)
Meagher (1975)	0.0328(4)	0.0503(4)	0.6534(5)	0.93(20)	0.40(6)	0.29(11)	0.47(11)
Hazen and Finger (1978)	0.0328(2)	0.0502(2)	0.6534(2)	0.70(5)	0.31(3)	0.32(3)	0.35(3)
This study	0.0329(2)	0.0501(2)	0.6528(2)	0.71(5)	0.36(3)	0.29(3)	0.29(4)
<b>Grossular (<math>Ca_3Al_2Si_3O_{12}</math>)**</b>							
Prandl (1966)	0.0381(1)	0.0458(1)	0.6512(1)	0.26(2)	0.20(3)	0.24(2)	0.22(2)
Prandl (1966) (neutron diffraction)	0.0384(1)	0.0457(1)	0.6511(1)	0.56(5)	0.31(7)	0.18(5)	0.33(2)
Novak and Gibbs (1971)	0.0381(1)	0.0449(1)	0.6514(1)	0.61(1)	0.66(2)	0.56(2)	0.76(2)
Meagher (1975)	0.0380(5)	0.0447(5)	0.6512(4)	0.39(10)	0.40(6)	0.30(11)	0.37(9)
Hazen and Finger (1978)	0.0380(1)	0.0450(1)	0.6518(1)	0.33(2)	0.25(1)	0.29(4)	0.35(2)
This study	0.0376(2)	0.0454(2)	0.6513(2)	0.32(2)	0.23(3)	0.27(3)	0.19(3)

\* Pyrope data from synthetic samples.

\*\* Grossular data from natural specimens, except this study.

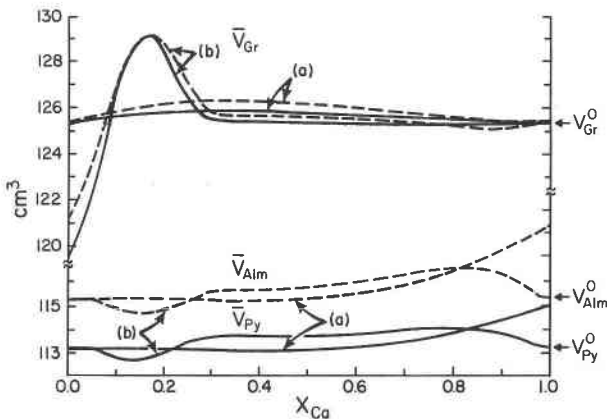


Fig. 7. Partial molar volumes of end-member components (12 O atom basis) in the pyrope-grossular (solid lines) and almandine-grossular (dashed lines) joins. (a) This study. (b) Cressey et al. (1978).

follows:

$$\Delta V^{xs} = X_{Ca}X_{Mg}(W_{CaMg}^V X_{Mg} + W_{MgCa}^V X_{Ca}) \quad (2)$$

where  $W_{CaMg}^V = 0.36 \pm 0.23$  and  $W_{MgCa}^V = 1.73 \pm 0.3$  cm<sup>3</sup>. The partial molar volumes of pyrope and grossular components, expressed as a function of composition according to standard thermodynamic principles (e.g., Ganguly and Saxena, 1987, p. 8), is as follows:

$$V_{Gr}(Gr-Py) = A + [W_{CaMg}^V + 2(W_{MgCa}^V - W_{CaMg}^V) \cdot X_{Ca}]X_{Mg}^2 \quad (3a)$$

$$V_{Py}(Gr-Py) = A + [W_{MgCa}^V + 2(W_{CaMg}^V - W_{MgCa}^V) \cdot X_{Mg}]X_{Ca}^2 \quad (3b)$$

where  $A = X_{Ca}V_{Gr}^0 + X_{Mg}V_{Py}^0$ .

Geiger et al. (1989) have determined the molar volume in the almandine-grossular join, which disagrees with the results of Cressey et al. (1978), but is very similar to the volumetric behavior of the pyrope-grossular join determined in this work. The partial molar volumes of grossular and almandine components derived from the data of Geiger et al. are as follows:

$$\bar{V}_{Gr}(Gr-Alm) = B + [W_{CaFe}^V + 2(W_{FeCa}^V - W_{CaFe}^V) \cdot X_{Ca}]X_{Fe}^2 \quad (4a)$$

$$\bar{V}_{Alm}(Gr-Alm) = B + [W_{FeCa}^V + 2(W_{CaFe}^V - W_{FeCa}^V) \cdot X_{Fe}]X_{Ca}^2 \quad (4b)$$

where  $B = X_{Ca}V_{Gr}^0 + X_{Fe}V_{Alm}^0$ ,  $W_{CaFe}^V = 0$ , and  $W_{FeCa}^V = 3.0$  cm<sup>3</sup>. The partial molar volumes of garnet components in the binary joins pyrope-grossular and almandine-grossular, as derived above, are illustrated in Figure 7 and compared with the results of Cressey et al. (1978), who derived these values from their own volume data on the almandine-grossular join and from the data of Newton et al. (1977) on the pyrope-grossular join.

Calculation of the equilibrium pressure of the assemblage garnet + aluminosilicate + plagioclase + quartz (GASP), which is one of the most extensively used geobarometers, requires data on the partial molar volume of the grossular component in multicomponent garnet. Natural garnets in the GASP assemblage have 2–18 mol% grossular (Newton and Haselton, 1981) and thus have  $\bar{V}_{Gr}$  values that are often significantly different from the molar volume of grossular, according to the data of Cressey et al. (1978) and Newton et al. (1977), but they are not so according to our data and those of Geiger et al. (1989). Since  $\bar{V}_{Gr}$  changes very little with the Fe/Mg ratio (Fig. 7), one would make a negligible error by setting  $\bar{V}_{Gr}$  in ternary Ca-Fe-Mg garnet equal to the weighted average of  $\bar{V}_{Gr}$  in the two limiting binary joins, as suggested by Newton and Haselton (1981). It can be easily shown, using the barometric expression of the GASP assemblage (e.g., Ganguly and Saxena, 1987, their Eq. 4.27), that even if the slight volumetric nonideality given by our data is completely neglected, one would underestimate the equilibrium pressure of the GASP assemblage by no more than 1.5%.

The partial molar volumes of almandine and pyrope components are essentially independent of grossular concentration up to ~50 mol% Ca, which covers most geologically important situations. For extremely Ca-rich compositions, such as in grosspydites (Sobolev et al., 1968), the partial molar volumes of almandine and pyrope depart significantly from their respective molar volumes. However, no correction for volumetric nonideality of garnet is needed for the calculation of the pressure effect on Fe-Mg exchange geothermometers, since the Ca has a very similar effect on the partial molar volumes of both pyrope and almandine components.

#### Elastic enthalpy of mixing

The process of formation of a solid solution [ $xA\phi + (1-x)B\phi \rightarrow (A_xB_{1-x})\phi$ ] can be formally thought to consist of the following steps (Ferreira et al., 1988): (1) change of the molar volumes of the end-member components to the molar volume  $V$  of the solid solution, i.e.,  $xV^0(A,\phi) \rightarrow xV$  and  $(1-x)V^0(B,\phi) \rightarrow (1-x)V$ , and (2) mixing of these components to form a chemically homogeneous mixture (which corresponds to spin-flips in classic Ising models). Steps (1) and (2) are often referred to as the elastic and chemical components of the enthalpy of mixing, respectively. Ferreira et al. (1988) have developed expressions to calculate the elastic effect and have shown that ignoring the effect of multiatom interaction leads to substantial overestimation of the elastic enthalpy of mixing. In the zeroth approximation, i.e., ignoring the effect of multiatom interaction, one has

$$\Delta H_{0,elast} = (1-x) \int_0^x XZ(X) dX + x \int_x^1 (1-X)Z(X) dX \quad (5a)$$

where

$$Z = \frac{B}{V} \left( \frac{dV}{dX} \right) \quad (5b)$$

and  $B$  is the bulk modulus. The subscript zero indicates zeroth approximation.

With a subregular expression for  $\Delta V^{ss}$  (Eq. 2),

$$\frac{dV}{dX} = (V_1^0 - V_2^0) + W_{12} + A_1 + A_2 \quad (6)$$

where

$$A_1 = 2(W_{21} - 2W_{12})X \text{ and } A_2 = 3(W_{12} - W_{21})X^2 \text{ and } X \equiv X_1.$$

Using Equations 5 and 6, and the volume data determined in this work (Eq. 2), we have calculated  $\Delta H_{0,elast}$  in the pyrope-grossular join. For simplicity, we have assumed that the ratio  $B/V$  changes linearly between the terminal compositions (a similar assumption was made by Ferreira et al., 1988). This assumption implies that the slope of  $V$ - $P$  curve at any  $P$ - $T$  condition changes linearly with composition. The bulk moduli for pyrope and grossular were taken from Leitner et al. (1980) and Bass (1989), respectively. The calculated elastic enthalpy can be represented by a subregular form,  $\Delta H = W(x)x(1-x)$ , where  $W(x) = W_{21}^0x + W_{12}^0(1-x)$ .

Following Ferreira et al. (1988), the effect of multiatom interaction can be incorporated as follows. If only nearest neighbor interactions are significant, and there are  $m$  (Mg + Ca) atoms in the nearest neighbor cell with subregular mixing behavior, then the net elastic enthalpy of mixing is given by

$$\Delta H_{elast} = W(x) \left[ x(1-x) - \sum_{n=0}^m P_n(x) X_n (1-X_n) \right] \quad (7)$$

where  $n = mx_c$ ,  $x_c$  being the cluster composition (so that  $0 \leq n \leq m$ ),  $X_n = n/m$ , and  $P_n(x)$  is the random probability for  $m$  atom clusters at a composition  $x$  of the solid solution. The second term in Equation 7 embodies the elastic effect of a medium-cluster interaction.

It can be shown (Appendix 1) that

$$\sum_{n=0}^m P_n(x) X_n (1-X_n) = \frac{m-1}{m} x(1-x) \quad (8)$$

so that

$$\begin{aligned} \Delta H_{elast} &= W(x) \left[ x(1-x) - \frac{m-1}{m} x(1-x) \right] \\ &= \frac{W(x)}{m} x(1-x) \\ &= \frac{\Delta H_{0,elast}}{m}. \end{aligned} \quad (9)$$

In other words, the net elastic enthalpy of mixing is lower by a factor of  $m$  (i.e., by the number of atoms in the nearest neighbor cell participating in solid solution) than that calculated in the zeroth approximation.

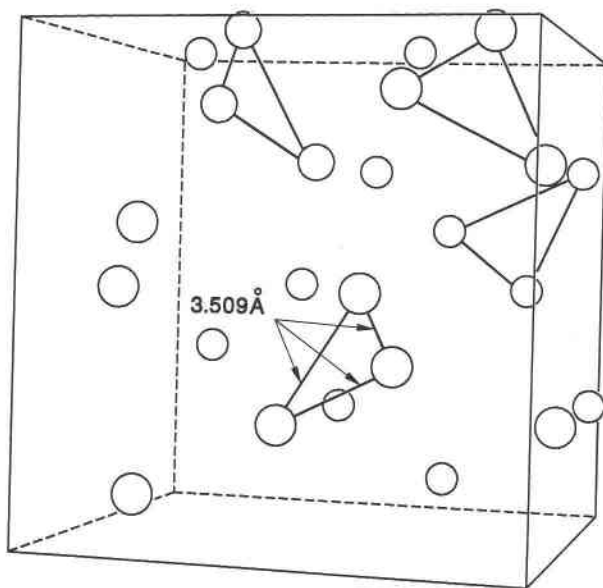


Fig. 8. Unit cell of pyrope showing only Mg atoms. The nearest neighbor Mg atoms, which are 3.509 Å apart, form triangular clusters.

In garnet, the divalent (dodecahedral) cations constitute triangular nearest neighbor cells. This is illustrated in Figure 8 by removing all but the Mg atoms from the unit cell of pyrope and rotating the unit cell arbitrarily for the sake of clarity. The drawing was done by using the program Atoms (Dowty, 1991: a computer program for displaying atomic structures), which is available commercially (copyright: Eric Dowty). The nearest neighbor Mg atoms, which are 3.509 Å apart, were identified by using the program Distance, written by Antonio della Guista of the University of Padova, Italy, and then joined together to form the nearest neighbor clusters (the next nearest neighbors are 5.36 Å apart).

Setting  $m = 3$ , we have calculated the elastic enthalpy of mixing in garnet according to Equations 5 and 9. The results are illustrated in Figure 9A; also shown for comparison is the  $\Delta H_{elast}$  if the  $V$ - $X$  relation in the pyrope-grossular join were ideal. Figure 9B shows a comparison of  $\Delta H_{elast}$  with the enthalpy of mixing calculated from the heat of solution measurement by Newton et al. (1977) of end-member and solid solutions in the pyrope-grossular join. The calorimetric enthalpy of mixing was calculated according to the procedure and weighting scheme suggested by Haselton and Newton (1980). These data, which form the basis of existing mixing models in the pyrope-grossular join (e.g., Ganguly and Saxena, 1987; Berman, 1990), lie close to the enthalpy of mixing calculated from the volume of mixing (elastic model), but have an asymmetry toward the opposite (i.e., pyrope) end. The reason for this difference in the nature of the asymmetry is not clear. The calorimetric enthalpy of mixing incorporates both chemical and elastic effects. Thus, the difference between the calorimetric and elastic enthalpy of mixing, including that in the nature of the asymmetry, may be

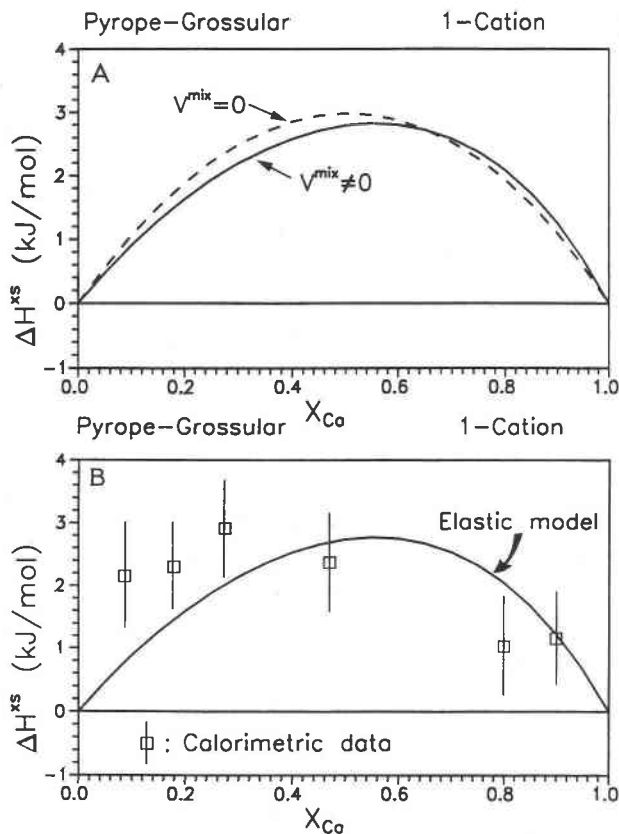


Fig. 9. (A) Effect of elastic strain energy on the enthalpy of mixing in the pyrope-grossular join. (B) Comparison of the elastic and calorimetric enthalpies of mixing. The calorimetric data are from Newton et al. (1977). Vertical bars:  $\pm 1\sigma$ .

due to chemical factors. We note, however, that all other binary joins in the garnet solid solution investigated so far (Mg-Fe: Hackler and Wood, 1989; Fe-Ca: Geiger et al., 1987) show maximum (net) positive deviation from ideality toward the larger cation, which is in contrast to the form of the calorimetric  $\Delta H$  data in the pyrope-grossular join.

#### Reciprocal solution effect and stability

The dependence of the octahedral bond distance on the size of the dodecahedral cation, as illustrated in Figure 6B, suggests that the mixing property of trivalent cations in the octahedral site of silicate garnet should, in principle, depend on the composition of dodecahedral site, and vice versa. As discussed by Ganguly and Saxena (1987), in the treatment of multisite or reciprocal solid solutions, this interdependence of the site mixing properties is usually ignored in the formulation of activity expression of macroscopic end-member components. Whether this effect is significant in multisite garnet solid solutions compared with the other effects, especially that arising from the standard free energy change of the reciprocal exchange reaction, remains to be seen.

In garnets formed under crustal conditions, the con-

centration of  $Fe^{3+}$  and  $Cr^{3+}$  in the octahedral site can always be expressed in terms of the andradite ( $Ca_3Fe_2Si_3O_{12}$ ) and uvarovite ( $Ca_3Cr_2Si_3O_{12}$ ) components, respectively. This is because  $Fe^{3+}$  and  $Cr^{3+}$  are too large for the octahedral site when the dodecahedral site is filled with the divalent cations Fe, Mg, and Mn. The required expansion of the octahedral site is achieved through the substitution of Ca in the dodecahedral site. It is only in mantle-derived garnets that we find  $^{60}Cr^{3+}$  partially decoupled from Ca. Here the high pressures facilitate substitution or squeezing of the relatively larger trivalent cations into the octahedral site. Ringwood (1977) has synthesized  $Mg_3Al_2Si_3O_{12}$ - $Mg_3Cr_2Si_3O_{12}$  (pyrope-knorringite) solid solutions at 60–80 kbar, 1400–1500 °C.

#### ACKNOWLEDGMENTS

This research was supported by a U.S. National Science Foundation grant no. EAR 8903995 and 9117927 to J.G. We are grateful to Antonio della Guista for his help in drawing Figure 8. Thanks are due to Benjamin Burton and an anonymous reviewer for their constructive comments, and to Luciano Ungaretti for comments and insightful discussions about the structural properties of garnets.

#### REFERENCES CITED

- Bass, J.D. (1989) Elasticity of spessartine garnets by Brillouin spectroscopy. *Journal of Geophysical Research*, 94, 7621–7628.
- Berman, R. (1990) Mixing properties of Ca-Mg-Fe-Mn garnets. *American Mineralogist*, 75, 328–344.
- Bevington, P.R.C. (1969) Data reduction and error analysis for the physical sciences, 336 p. McGraw-Hill, New York.
- Boyd, F.R. (1970) Garnet peridotites and the system  $CaSiO_3$ - $MgSiO_3$ - $Al_2O_3$ . *Mineralogical Society of America Special Paper*, 3, 63–75.
- Cressey, G., Schmid, R., and Wood, B.J. (1978) Thermodynamic properties of almandine-grossular garnet solid solutions. *Contributions to Mineralogy and Petrology*, 67, 397–404.
- Delaney, J.M. (1981) A spectral and thermodynamic investigation of synthetic pyrope-grossular garnets, 201 p. Ph.D. thesis, University of California, Los Angeles, California.
- Dowty, E. (1991) ATOMS: A computer program for displaying atomic structures. Copyright E. Dowty, 521 Hidden Valley Road, Kingsport, Tennessee 37663, USA.
- Ferreira, L.G., Mbaye, A.A., and Zunger, A. (1988) Chemical and elastic effects on isostructural phase diagrams: The  $\epsilon$ -G approach. *Physical Review B*, 37, 10547–10570.
- Ganguly, J., and Saxena, S.K. (1984) Mixing properties of aluminosilicate garnets: Constraints from natural and experimental data, and applications to geothermo-barometry. *American Mineralogist*, 69, 88–97.
- (1987) *Mixtures and mineral reactions*, 291 p. Springer-Verlag, Berlin.
- Gasparik, T. (1984) Experimentally determined stability of clinopyroxene + garnet + corundum in the system  $CaO$ - $MgO$ - $Al_2O_3$ - $SiO_2$ . *American Mineralogist*, 69, 1025–1035.
- Geiger, C.A., Newton, R.C., and Kleppa, O.J. (1987) Enthalpy of mixing of synthetic almandine-grossular and almandine-pyrope garnets from high temperature solution calorimetry. *Geochimica et Cosmochimica Acta*, 51, 1755–1763.
- Geiger, C.A., Winkler, B., and Langer, K. (1989) Infrared spectra of synthetic almandine-grossular and almandine-pyrope solid solutions: Evidence for equivalent site behavior. *Mineralogical Magazine*, 53, 231–237.
- Gibbs, G.V., and Smith, J.V. (1965) Refinement of the crystal structure of synthetic pyrope. *American Mineralogist*, 50, 2023–2039.
- Hackler, R.T., and Wood, B.J. (1989) Experimental determination of Fe and Mg exchange between garnet and olivine and estimation of Fe-Mg garnet mixing properties. *American Mineralogist*, 74, 994–999.
- Haselton, H.T., and Newton, R.C. (1980) Thermodynamics of pyrope-

grossular garnets and their stabilities at high temperatures and pressures. *Journal of Geophysical Research* (G.C. Kennedy volume), 85, 6973-6982.

Hazen, R.M., and Finger, L.W. (1978) Crystal structures and compressibilities of pyrope and grossular to 60 kbar. *American Mineralogist*, 63, 297-303.

Leitner, B.J.D., Weidner, J., and Liebermann, R.C. (1980) Elasticity of single crystal pyrope and implications for garnet solid solution series. *Physics of the Earth Planetary Interiors*, 22, 111-121.

Meagher, E.A. (1975) The crystal structure of pyrope and grossularite at elevated temperatures. *American Mineralogist*, 60, 218-228.

Newton, R.C., and Haselton, H.T. (1981) Thermodynamics of the garnet-plagioclase-Al<sub>2</sub>SiO<sub>5</sub>-quartz geobarometer. *Advances in Physical Geochemistry*, 1, 131-147.

Newton, R.C., and Wood, B.J. (1980) Volume behavior of silicate solid solutions. *American Mineralogist*, 65, 733-745.

Newton, R.C., Charlu, T.V., and Kleppa, O.J. (1977) Thermochemistry of high pressure garnets and clinopyroxenes in the system CaO-MgO-Al<sub>2</sub>O<sub>3</sub>-SiO<sub>2</sub>. *Geochimica et Cosmochimica Acta*, 41, 369-377.

Novak, G.A., and Gibbs, G.V. (1971) The crystal chemistry of the silicate garnets. *American Mineralogist*, 56, 791-825.

O'Neill, H.St.C., Dollase, W.A., and Ross II, C.R. (1991) Temperature dependence of the cation distribution in nickel aluminate (NiAl<sub>2</sub>O<sub>4</sub>) spinel: A powder XRD study. *Physics and Chemistry of Minerals*, 18, 302-319.

Prandl, W. (1966) Verfeinerung der Kristallstruktur des Grossulars mit Neutronen- und Röntgenstrahlbeugung. *Zeitschrift für Kristallographie*, 123, 81-116.

Ringwood, A.E. (1977) Synthesis of pyrope-knorringite solid solutions. *Earth and Planetary Science Letters*, 36, 443-448.

Sobolev, V.N., Jr., Kuznetsova, I.K., and Zyuzin, N.I. (1968) The petrology of grosspyrite xenoliths from zagadochnaya kimberlite pipe in Yakutia. *Journal of Petrology*, 9, 253-280.

Wiles, D.B., and Young, R.A. (1981) A new computer program for Rietveld analysis of X-ray powder diffraction patterns. *Journal of Applied Crystallography*, 14, 149-151.

Wood, B.J. (1988) Activity measurements and excess entropy-volume relationships for pyrope-grossular garnets. *Journal of Geology*, 96, 721-729.

MANUSCRIPT RECEIVED AUGUST 11, 1992

MANUSCRIPT ACCEPTED JANUARY 8, 1993

### APPENDIX 1: DERIVATION OF THE EFFECT OF MEDIUM-CLUSTER INTERACTION ON THE ENTHALPY OF MIXING (SEE TEXT, EQ. 8)

Let us consider a solid solution ( $A_x B_{1-x}$ )C in which the nearest neighbor cell consists of  $m(A + B)$  atoms. Let  $x_c$  be the fractional concentration of A in an  $m$ -atom cluster. The composition of such a cluster can also be expressed as ( $A_n B_{m-n}$ )C<sub>m</sub> where  $n = mx_c$  (so that  $0 \leq n \leq m$ ). The random probability for  $m$ -atom clusters of composition  $x_c$  is given by (Ferreira et al., 1988):

$$P_n(x) = (C_n^m) x^n (1-x)^{m-n}. \quad (\text{A1})$$

Consequently, the second term within the square bracket of Equation 7, which accounts for the effect of medium-cluster interaction, can be expressed as follows:

$$\sum_{n=0}^m P_n(x) X_n (1 - X_n)$$

$$\begin{aligned} &= \sum_{n=0}^m \frac{m!}{n!(m-n)!} x^n (1-x)^{m-n} \cdot \frac{n}{m} \binom{m-n}{m} \\ &= \sum_{n=0}^m \frac{(m-1)!}{(n-1)!(m-n-1)!} x^n (1-x)^{m-n} \left(\frac{1}{m}\right). \quad (\text{A2}) \end{aligned}$$

The first and last terms in the above summation equal zero. Thus,

$$\begin{aligned} &\sum_{n=0}^m P_n(x) X_n (1 - X_n) \\ &= \sum_{n=1}^{m-1} \frac{(m-1)!}{(n-1)!(m-n-1)!} x^n (1-x)^{m-n} \left(\frac{1}{m}\right) \\ &= \frac{(m-1)!}{(m-2)!} x (1-x)^{m-1} \cdot \frac{1}{m} \\ &\quad + \frac{(m-1)!}{1!(m-3)!} x^2 (1-x)^{m-2} \cdot \frac{1}{m} \\ &\quad + \frac{(m-1)!}{2!(m-4)!} x^3 (1-x)^m + \dots \\ &\quad + \frac{(m-1)!}{(m-4)!2!} x^{m-3} (1-x)^3 \cdot \frac{1}{m} \\ &\quad + \frac{(m-1)!}{(m-3)!1!} x^{m-2} (1-x)^2 \cdot \frac{1}{m} \\ &\quad + \frac{(m-1)!}{(m-2)!} x^{m-1} (1-x) \cdot \frac{1}{m} \\ &= \frac{(m-1)!}{(m-2)!m} x (1-x) \\ &\quad \cdot \left[ (1-x)^{m-2} + \frac{(m-2)!}{1!(m-3)!} x (1-x)^{m-3} \right. \\ &\quad + \frac{(m-2)!}{2!(m-4)!} x^2 (1-x)^{m-4} + \dots \\ &\quad + \frac{(m-2)!}{(m-4)!2!} x^{m-4} (1-x)^2 \\ &\quad \left. + \frac{(m-2)!}{(m-3)!1!} x^{m-3} (1-x) + x^{m-2} \right] \\ &= \frac{m-1}{m} x (1-x) [(1-x)^{m-2} + C_{m-2}^1 x (1-x)^{m-3} \\ &\quad + C_{m-2}^2 x^2 (1-x)^{m-4} + \dots \\ &\quad + C_{m-2}^{m-4} x^{m-4} (1-x)^2 \\ &\quad + C_{m-2}^{m-3} x^{m-3} (1-x) + x^{m-2}]. \quad (\text{A3}) \end{aligned}$$

Noting that the terms within the square brackets of Equation A3 represent a binomial expansion of  $[(1-x) + x]^{m-2}$ , which is unity, we have

$$\sum_{n=0}^m P_n(x) X_n (1 - X_n) = \frac{m-1}{m} x (1-x). \quad (\text{A4})$$